Predictive Models of Nanodevices

Dalibor Biolek, *Senior Member, IEEE*, and Zdeněk Biolek

***Abstract*—Chua's concept of nonlinear higher-order elements is generalized with the aim of extending the procedures of predictive modeling of complex electrical systems to various nonelectrical domains. Special attention is paid to nanodevices with ambiguous hysteretic characteristics and their predictive modeling via unambiguous constitutive relations. It is shown on an example of spin-torque nano-oscillator how its Newton-like equation of motion can be used for constructing the predictive model of this device, and how this model can be useful for identifying the mechanisms of the oscillator dynamics.**

***Index Terms*—Predictive model, constitutive relation, nonlinear element, higher-order element, Chua's table, storeyed structure, memristor, pinched hysteresis loop.**

I. Introduction

MANY molecular and nanoscale electronic devices and components have been proposed or manufactured so far, from those composed of nanowires, carbon nanotubes or nanoparticles to ion-sensitive field-effect transistors and molecular switches. The quantum-electrical and other phenomena, which are not the cup of tea of current CMOS designers, may stay behind the mechanism of their operation, hence they should be allowed in realistic modeling and analysis of nanoscale devices. From among several simple examples where the standard formulae fail in the nanoscale, let us mention the regularities governing the capacitance/inductance of nano-sized capacitor [1] /inductor [2]. The very first models of the so-called HP memristor, based on the simple idea of the boundary between conducting and insulating regions of titanium dioxide moving after the application of an external bias voltage across the device [3], did not reflect correctly both the complex behavior and the physical mechanism of the operation of this device. They were subsequently substituted by quite different and more sophisticated models, taking into account the tunneling effects in Metal-Insulator-Metal (MIM) junction [4], thermally activated conducting filaments [5], and other mechanisms.

On the other hand, the consistent circuit-theoretic analysis, starting from the classical theory of nonlinear dynamic systems, and systematically applied to the nanoscale, can be useful in demystifying several phenomena hitherto observable in nanodevices, neuromorphic circuits, or, for example, in living cells. It is demonstrated in [6] that the concepts of local activity [7], edge of chaos [8], or Chua's table of higher-order elements [9] can explain the peculiar behavior of the ionic channels of the Hodgkin-Huxley axon [10], pinched hysteresis of nanowires [11], or a current passing through the Josephson junction due to interference among quasi-particle pairs [12].

Such a synergy of the classical and quantum-mechanical or quantum-electrical analyses, leading to more realistic and effective modeling of nanodevices, is possible with the help of Chua's concept of the so-called predictive modeling [6]. In 1980, Chua introduced hypothetical two-terminal building blocks, the (α, β) higher-order elements, each being represented by its special, generally nonlinear mathematical model with predicting ability, the so-called constitutive relation between two variables of the element, namely the integer-order integral/derivative of terminal voltage and current [9]. The classical resistor, capacitor, inductor, and their memory versions, memristor, memcapacitor, and meminductor form a small subset of these classes of fundamental two-terminal elements, organized in Chua's table. According to [6], the significance of these elements is that "*realistic circuit models of all current and future molecular and nanodevices must necessarily build upon these building blocks*". In other words, predictive models of existing devices must be composed of higher-order elements with predictive properties.

On the other hand, however, it is known that only a small subset of all general systems can be synthesized using only two-terminal elements. It is emphasized in [9] that "..*it is generally impossible to model an* $(n + 1)$*-terminal or n-port device using only* 2*-terminal elements as building-blocks*". The above idea of two-terminal fundamental elements can be therefore generalized to multipoles or multiports [13]. The so-called algebraic n-ports, whose subset are the memristive n-ports, can be mentioned as a typical example [13]. As another generalization, Chua's table was extended by fractional-order elements [14].

No matter if the above elements are two-terminal elements or n-ports of integer or fractional order, they are significant building blocks for generating predictive models of nano-devices.

Chua shows a lot of examples, particularly from biophysics journals, of models with mistaken identity, when the analyzed system or phenomenon is described by a model without predictive ability. Such a model can be, for example, in the form of multivalued characteristic (see the pinched hysteresis loops of resistive switching memories; the loop form depends on the way of the device excitation), or frequency-dependent models (for example a nanocoil made from BC_2N nanotubes modeled by LR cell with frequency-dependent inductance and resistance

Manuscript received July 31, 2017; revised December 19, 2017; accepted February 25, 2018. Date of publication April 9, 2018; date of current version September 6, 2018. This work was supported by Czech Ministry of Education in frame of National Sustainability Program under Grant LO1401. For research, infrastructure of the SIX Center was used. The review of this paper was arranged by the MEMRISYS 2017 Guest Editors. *(Corresponding author: Dalibor Biolek.)*

D. Biolek is with the Department of Microelectronics, Brno University of Technology, Brno 616 00, Czech Republic, and also with the Department of Electrical Engineering, University of Defence, Brno 602 00, Czech Republic (e-mail: dalibor.biolek@unob.cz).

Zdeněk Biolek is with the Department of Microelectronics, Brno University of Technology, Brno 616 00, Czech Republic (e-mail: zdenek.biolek@gmail.com).

Digital Object Identifier 10.1109/TNANO.2018.2812359

[2], or the multi wall carbon nano-tube inductor [15] and inductor using the nano-granular magnetic core [16] exhibiting frequency-dependent quality factor). Similar models are generated via today popular methods of electrochemical impedance spectroscopy (EIS) of tissues, living or fuell cells [17], [18]. They are not predictive because their validity is limited to small-signal excitation about the DC bias. In fact, the final models can be derived from more complex nonlinear models. However, their derivation is much more complicated. The presence of linear R, C, and L elements with frequency-dependent parameters may be another sign of incorrect modeling, because such elements can be only small-signal models of nonlinear higher-order elements. The exotic Warburg impedance, which is a part of the today standard small-signal Randles model of an electrode-electrolyte interface (EEI) [19], is a non-predictive small-signal CPE (Constant Phase Element) model of the nonlinear fractional-order element. The mistaken frequency-dependent model of chiral conducting nanotube in [2] can be re-designed as a series circuit made up of several higher-order elements [6]. The famous Hodgkin–Huxley circuit model, describing the ionic mechanism of the initiation and propagation of the action potential in neurons, uses time-varying resistors for modeling potassium and sodium channels [20]. It is shown in [10] that these channels behave in fact as locally-active memristors. Such predictive modeling enables us to explain several hitherto pending phenomena associated with the behavior of neuron cells such as anomalous inductance, hysteretic behavior or the mechanism of generating the action potentials [6].

As a frequent source of misunderstanding, the hypothetical element from Chua's table for predictive modeling of existing objects is usually replaced by the object being modeled. For example, the nanodevice, fabricated in Hewlett-Packard labs [3] and frequently denoted as HP or TiO_2 memristor, is in fact a nonlinear two-terminal device whose behavior can be modeled by the (–1, –1) higher-order element called memristor only roughly.

As regards various two-terminal devices, which exhibit the hysteresis loops pinched at the *v*–*i* origin under their periodical excitation, such as resistive switching memories, phase-change and magnetoresistive RAM or Metal-Insulator-Metal (MIM) memory cells, they are often denoted as memristors [21] according to the principle "*If it's pinched it's a memristor*" [22]. As an additional experimental test supporting the hypothesis that the device is a memristor, the hysteresis loop must shrink with increasing the frequency towards infinity. In fact, it is a fingerprint of the memristor as a hypothetical higher-order element, which can be used, from among more such elements, to model important properties of this device. This fingerprint then manifests itself in the behavior of the device via its model.

Paradoxically, also the newly introduced classification of memristors contributes to blurring the otherwise obvious boundary between the hypothetical circuit elements for modeling and the existing devices. The original classification into memristors (in the sense of axiomatic definition of a hypothetical fundamental (α, β) higher-order element, where $\alpha = \beta = -1$) and general memristive systems [23] (all systems with the memristance as a function of internal state variables and voltage or current) is newly replaced by a classification into ideal memristor (which is the original memristor according to [24]) and extended memristor (which is the original memristive system), with "intermediate" ideal generic memristor and generic memristor. Their exact definitions can be found in [25], [26]. This novel classification legitimizes utilizing the term memristor to denote various memristive systems, although these models do not exhibit the behavior of the memristor as a fundamental element from Chua's table.

Chua's table contains the basic building blocks for generating predictive models. The memristor occupies therein its unique place with the coordinates (–1, –1). Nevertheless, some other types of memristor as building cells of more complicated nanosystems are defined, namely the higher-order memristors [14] and, particularly, the so-called inverse memristors [27]. With a view to the authors of this paper, such activities may bring confusion into the logic order built by L. Chua in the eighties of the last century.

The paper has three objectives: 1) To draw attention to the usefulness and timeliness of the predictive modeling of nanodevices. 2) To propose tools for revealing non-predictive models and models with mistaken identities. 3) To explain the corresponding approaches on concrete example.

In the following, Chua's concept of higher-order elements is summarized, with Chua's table and storeyed structure containing these electrical elements. Chua's table and the storeyed structure are then generalized to other nonelectrical domains with the aim to have, for example, a tool for predictive modeling of mechanical nanosystems (nano-springs [28], nano-dampers [29], nano-pendulum [30], nano-oscillators [31] etc.). Reference is made to some connections between the circuit variables used for modeling the element, their position in the storeyed structure, the small-signal parameters of the element, and the possibility of the appearance of hysteretic behavior as a sign of non-predictive modeling, including the frequency dependence of this hysteresis. The positions of the so-called higher-order memristors [14] in the classical storeyed structure are identified, hereby demonstrating that it is only a special name for already existing higher-order elements. The spin-torque nano-oscillator [31] is analyzed and its predictive model is found, compounded from the fundamental elements of Chua's table.

II. Building Blocks of Predictive Modeling

According to [6], the so-called higher-order (α, β) elements, organized in a table illustrated in Fig. 1(a), can serve as fundamental blocks for modeling nonlinear systems. The (α, β) element is defined via its, in general nonlinear, constitutive relation (CR) *F*() of the type

$$F(v^{(\alpha)}, i^{(\beta)}) = 0 \tag{1}$$

where the symbols $v^{(\alpha)}$ and $i^{(\beta)}$ with the integers α and β denote α and β multiple time-domain derivatives (for positive indices) or integrals (for negative indices) of voltage *v* and current *i*. Fig. 1(b) shows the positions of classical R, C, and L elements and their memory versions in the table, together with their codes

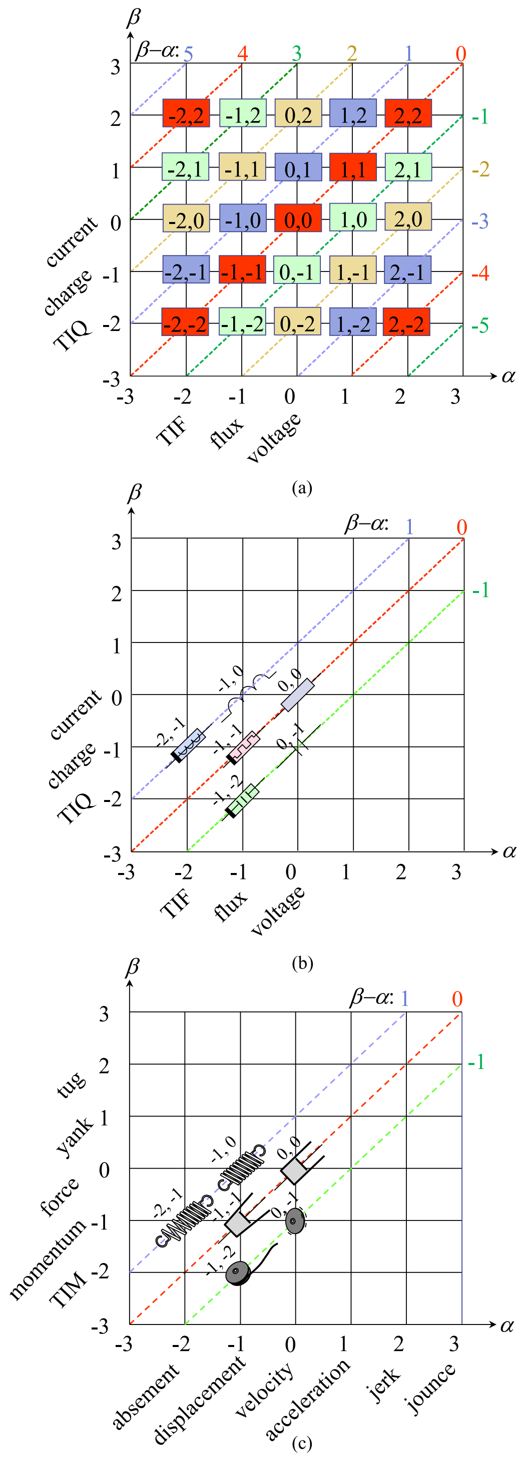

Fig. 1. (a) Part of Chua's table of electrical (α, β) higher-order elements. The difference β-α determines the type of small-signal model (-1 = capacitive, 0 = resistive, 1 = inductive, etc., see [6] for details). (b) Positions of resistor $(0, 0)$, capacitor $(0, -1)$, inductor $(-1, 0)$, memristor $(-1, -1)$, memcapacitor $(-1, -2)$, and meminductor $(-2, -1)$. Flux and charge denote time integrals of voltage and current, TIF and TIQ are time integrals of flux and charge. (c) Example of Chua's table for mechanical translational systems (the table is created via the analogies voltage ↔ velocity, current ↔ force). The corresponding time integrals and derivatives of the velocity and force are denoted according to [32]. TIM is the time integral of momentum. According to this analogy, mechanical resistor, capacitor, and inductor are damper, mass, and spring, respectively. Examples of their memory versions can also be found, for example spring with mechanical memory as mechanical meminductor or yo-yo toy as mechanical memcapacitor.

(α, β). The remaining higher-order elements have so far been discussed only marginally.

The following items should be noted with respect to the constitutive relation (1): 1) It is an *algebraic* relation between the corresponding constitutive variables, which does not depend on the environment of the element. The CR is therefore a predictive model of the element. 2) The CR (1) is generally nonlinear. 3) No (α, β) element can be obtained from the remaining elements. 4) The elements from Chua's table, each having its predictive model, can be used for building up more complicated systems with predictive models. 5) Most higher-order elements, which model existing devices or phenomena, are $v^{(\alpha)}$– or $i^{(\beta)}$–controlled. Then (1) can be written as an explicit function of $v^{(\alpha)}$ or $i^{(\beta)}$. 6) Linearizing the CR (1) about the operating point Q, the corresponding linear element has the impedance $Z_Q = s^{(\beta-\alpha)} m_{\mathrm{Q}}$, where *s* is the Laplace operator and m_{Q} is the slope of the characteristic $v^{(\alpha)}(i^{(\beta)})$ at the operating point Q [6].

It follows from the last item that the frequency characteristic of the small-signal model is governed by the difference $(\beta$-$\alpha)$ or by the position of the element on the corresponding diagonal in Chua's table. For example, all elements located on the diagonal $(\beta - \alpha) = 1$ exhibit small-signal inductive reactance. However, only one element, namely (–1, 0), is an inductor.

Furthermore, in the case of *linear* constitutive relations, all the elements from a given diagonal would exhibit equivalent behavior. Then, for example, there is no point in distinguishing between the resistor and memristor. The main strength of Chua's table is its potency to model complex nonlinear systems.

With the help of well-known analogies, the concept of the predictive modeling can be extended beyond electrical engineering. For modeling the nanomechanical devices, the Through and Across analogy is useful since it preserves the duality of the electrical and mechanical networks [32]. The across variable (A) appears across the two terminals of an element (voltage for electrical domain, linear or angular velocity for mechanical translation or rotation systems), whereas the through variable (T) passes through (current for electrical elements, force or torque for mechanical translation or rotation systems). The corresponding Chua table of mechanical elements is in Fig. 1(c).

Fig. 2 shows the so-called storeyed structure [33] as an equivalent representation of Chua's table. Its basement grows from the level of the Across and Through variables. Above/below are the levels of their time-domain integrals/derivatives. In some cases, the storeyed structure can be more illustrative than Chua's table since it strictly separates the "ground floor" with classical R, C, and L elements from the "first floor" occupied by their memory versions. Since the nature of the small-signal model of the element depends on the difference $(\beta$–$\alpha)$, it is obvious that the elements with rather "exotic" small-signal impedances, for example of the ω^{-3} type, must be located simultaneously on more floors. It will be shown below that the storeyed structure can also be useful for a descriptive analysis of hysteretic effects.

It should be noted that the so-called 2nd-order memristor is introduced in [14] via a constitutive relation between the integral of flux (TIF) and integral of charge (TIQ). As follows from Fig. 2, it is the (–2, –2) element. Similarly, the 3rd-order

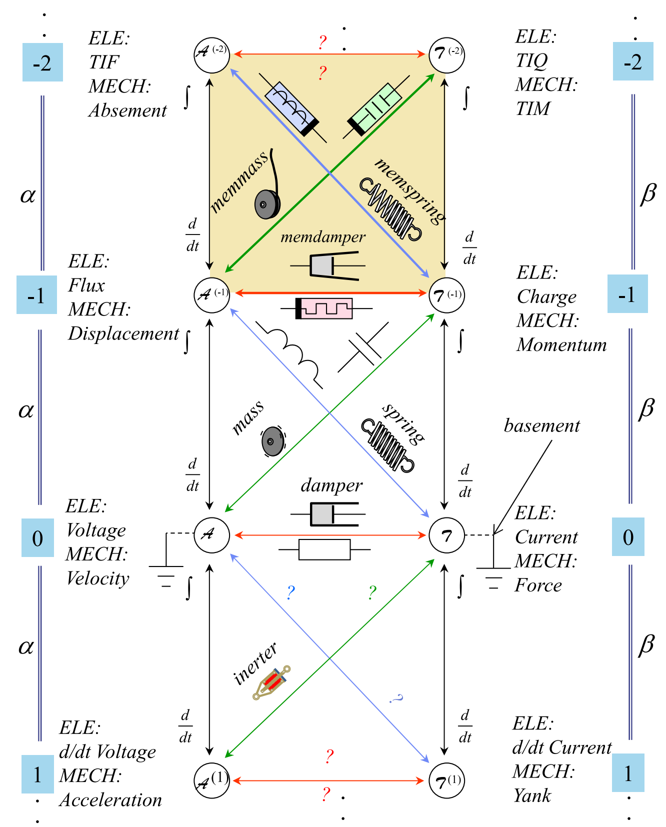

Fig. 2. Three floors of the storeyed structure with across and through basement, derived from generalized Chua's table. The "ground-floor" and "first-floor" are occupied by classical R, C, and L (or damper, mass, spring) elements and their memory versions. The "inter-floor" elements such as TIF-current are not displayed here. The newly discovered mechanical inerter [34] with its acceleration-force constitutive relation appears below the basement. The elements denoted by the question mark have not yet their names.

memristor, described in [14], is the (–3, –3) element, and other elements defined in [14], namely the 2nd-order memcapacitor and meminductor are classical (–2, –3) and (–3, –2) elements.

III. Hysteretic Characteristic of the Element as its Non-Predictive Model

The following statement is proved in [35]:

"The movement of the operating point of an arbitrary (α, β) element from Chua's table in the ($v^{(\alpha)}$, $i^{(\beta)}$) space, i.e., in the space of its nonlinear constitutive relation, is automatically accompanied by drawing a hysteresis loop pinched at the origin of the ($v^{(\alpha+1)}$, $i^{(\beta+1)}$) space. The true cause of the hysteresis is the nonlinearity of the constitutive relation of the element."

In other words, every nonlinear (α, β) element should be modeled via its constitutive relation, thus on that level of the storeyed structure on which it is located. Its prospective definition via the "one floor below" variables leads to the non-predictive hysteretic model. An illustrative example is the memristor, correctly modeled in the flux-charge coordinates whereas its model in the classical voltage-current space generates pinched hysteresis loops.

Fig. 3 explains the use of the storeyed structure for a simple analysis of the frequency dependence of the area of the *v*–*i* pinched hysteresis loop generated by the memristor. Fig. 3(a) shows the excitation by not commonly considered flux waveform (the memristor is driven at its definition level). Due to nonlinear constitutive relation of the memristor, the charge waveform $i^{(-1)}$ is distorted. This phenomenon together with the differentiation of the flux and charge waveforms generates the *v*–*i* hysteresis loop [35]. The second effect of the differentiation is a signal amplification, which is proportional to the first power of frequency. As a result, if the frequency increases, the hysteresis loop proportionally increases its size in the directions of both axes *v* and *i*, and its area therefore increases with the power of frequency [35].

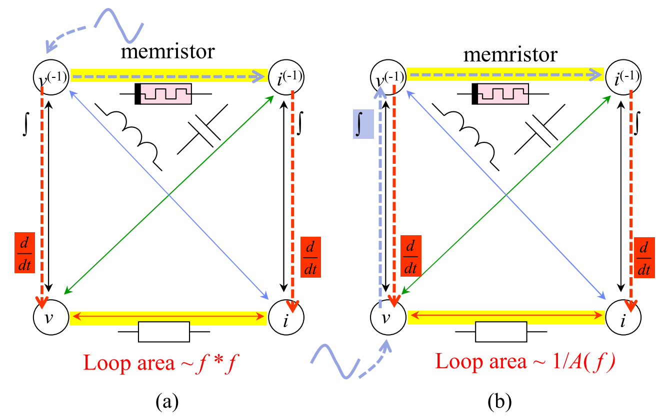

Fig. 3. Analysis of the frequency dependence of the area of pinched hysteresis loop of the memristor driven by (a) flux and (b) voltage.

Fig. 3(b) illustrates the commonly studied case of the memristor excitation by a voltage waveform. Since the memristance is controlled by a flux, and the voltage is transformed into the flux by time integration, the strength of this control diminishes proportionally with increasing frequency. In the limit case when $f \rightarrow \infty$, the operating point stops its movement along the nonlinear constitutive relation, and the memristor behaves as a linear resistor, thus without the *v*-*i* hysteresis. The area of the loop must therefore tend to zero with increasing frequency along a function 1/*A*(*f*) which depends on a concrete constitutive relation of the memristor and also on the initial position of the operating point. This trend cannot be overruled by the "amplifying" derivative elements in Fig. 3(b).

This simple methodology can be also used for explaining the peculiar behavior of circuits with mistaken identities [27].

IV. Example of Predictive Modeling—The Spin-Torque Nano-Oscillator

In [31], the authors analyze the dynamics of spin transfer nano-oscillators with an in-plane magnetized spin polarizer and magnetized free layer, separated by a thin non-magnetic spacer according to Fig. 4. The dynamic magnetization model, governed by the Landau-Lifshitz-Gilbert equation, was transferred to a model in the form of non-conservative Newton-like equation of motion

$$\frac{\ddot{\phi}}{\omega_p} + \alpha_{\text{eff}}\left(\phi\right)\dot{\phi} = -\frac{d\varepsilon_{\text{eff}}}{d\phi} \tag{2}$$

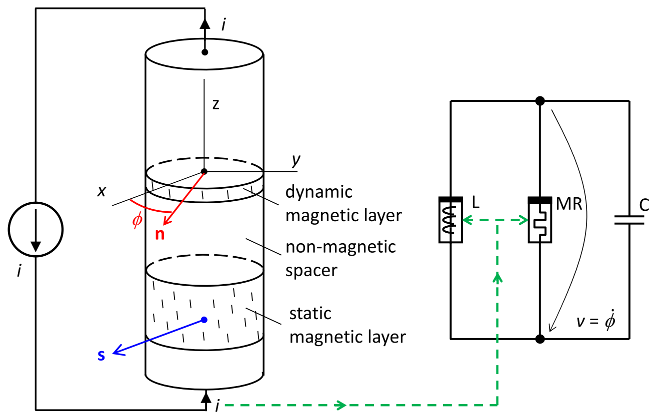

Fig. 4. (a) Spin-torque oscillator (STO) [31]. Static magnetic layer has a fixed magnetic moment with its direction given by the vector **s**, while the moment of the dynamic layer in the direction of the vector **n** moves in the easy plane anisotropy in the (*x, y*) plane. (b) Electric predictive model of the STO consisting of nonlinear inductor (L), nonlinear memristor (MR), and linear capacitor (C) in parallel. The constitutive relations of the L and MR depend on the electric current *i*.

for an "effective particle" with a mass of $1/\omega_p$ moving in the potential $\varepsilon_{\text{eff}}(\phi) = -0.5(\omega_a + u^2/\omega_p)\cos^2\phi - h\cos\phi$ with a variable friction coefficient $\alpha_{\text{eff}}(\phi) = \alpha + (2u/\omega_p)\cos\phi$. Here ϕ is the in-plane (azimuthal) polar angle measured from the *x*-axis, the constants ω_a, ω_p and h have the dimensions of frequency, and the spin transfer strength u is the rescaled driving current i. The symbol α denotes the Gilbert damping constant.

We demonstrate that the predictive model of this nano-oscillator can be built of three higher-order elements from the storeyed structure as is indicated in Fig. 4(b). Both electrical and mechanical models are derived below.

Consider a nonlinear memristor MR, capacitor C and inductor L in parallel. Let the constitutive relations of the MR, C and L elements be modeled by the nonlinear functions

$$\text{MR}: q_{\text{MR}} = q_{\text{MR}}(\varphi_{\text{MR}}), \text{C}: q_C = q_C(v_C), \text{L}: i_{\text{L}} = i_{\text{L}}(\varphi_{\text{L}}) \tag{3}$$

Then the equation of the circuit will be as follows:

$$\frac{dq_{\text{MR}}(\varphi)}{dt} + \frac{dq_c(\dot{\varphi})}{dt} + i_L(\varphi) = 0 \tag{4}$$

where $\dot{\varphi} = v$ is the voltage across the elements.

Equation (4) can be arranged to the form

$$G_M(\varphi)\dot{\varphi} + C^d(\dot{\varphi})\ddot{\varphi} + i_L(\varphi) = 0 \tag{5}$$

where

$$G_M(\varphi) = \frac{dq_{\text{MR}}(\varphi)}{d\varphi}, C^d(v) = \frac{dq_c(v)}{dv}, v = \dot{\varphi} \tag{6}$$

are the memductance G_M and differential capacitance C^d.

Equation (5) can be compared with the equation of motion of the oscillator (2) modified to the form

$$\frac{1}{\omega_p}\ddot{\phi} + \left(\alpha + \frac{2u}{\omega_p}\cos\phi\right)\dot{\phi} + \frac{1}{2}\left(\omega_a + \frac{u^2}{\omega_p}\right)\sin 2\phi + h\sin\phi = 0 \tag{7}$$

As follows from the electro-rotational-mechanical analogies, the voltage corresponds to the angular velocity and the flux φ to the angle ϕ. The predictive electric model of the nano-oscillator therefore consists in a parallel configuration of memristor, linear capacitor, and nonlinear inductor, with the following characteristics:

$$G_M(\varphi) = \alpha + \frac{2u}{\omega_p}\cos\varphi, C = C^d = \frac{1}{\omega_p},$$
$$i_L(\varphi) = \frac{1}{2}\left(\omega_a + \frac{u^2}{\omega_p}\right)\sin 2\varphi + h\sin\varphi \tag{8}$$

A comparison of (2), (7) and (8) shows that the angle-dependent friction coefficient α_{eff} and the flux-dependent memductance G_M of the memristor are expressed by identical terms. The friction coefficient, dependent on the position (angle ϕ), is a sign of memristive damping, reported for the first time by Oster and Auslander [36]. The oscillator can therefore be modeled by a resonant circuit whose immediate damping is given by the instantaneous value and sign of the memristor conductivity. The $G_M(\varphi)$ function (memductance or memory conductivity) governs the behavior of the "effective particle" near the equilibrium points of the potential field ε_{eff}.

The functional rule for the gradient of ε_{eff} is identical to the constitutive relation of the nonlinear inductor. As follows from (8), both the inductor and memristor characteristics are modulated by external excitation u.

The corresponding mechanical model consists of a nonlinear rotational damper with the mem-damping $b = G_M(\phi)$, linear inertia (mass) element with the moment of inertia $I = C$, and nonlinear elastic shaft (spring) with the constitutive relation between torque and angle of rotation $T(\phi) = 0.5(\omega_a + u^2/\omega_p)\sin 2\phi + h\sin\phi$.

The above STO model in Fig. 4(b) can be easily implemented in SPICE-like programs and utilized for an effective simulation in various application circuits without the necessity of time-consuming numerical computation of the original vector-type Landau-Lifshitz-Gilbert equation [31].

The results of the simulation of the single STO are given in Figs. 5 and 6. The parameters are set for the so-called small field case, i.e., $h < \omega_a + u^2/\omega_p$ [31]. The graphs in Fig. 5(a)–(c) represent the waveforms of the angle ϕ and the angular velocity $d\phi/dt$, and Fig. 6(a)–(c) shows the corresponding movements of the "effective particle" in the potential fields ε_{eff}. The model works with the scaled variables $r_h = h/\omega_a$, $r_p = \omega_p/\omega_a$, and $r_u = u/\omega_a$. Fig. 6 shows that the profile of ε_{eff} depends on the excitation r_u. The period of small oscillations ① and full rotations ③ is 111.2 psec. and 110.8 psec., respectively. The oscillator behavior is also determined by its initial angle ϕ_0, which can determine the final regime of the oscillator or into which of the two neighboring potential well it will get. The simulations show that the small oscillations can occur for r_u ranging from -0.050 to -0.0757 with the oscillation period from 82.0 psec. to 475.1 psec. When r_u is reduced to -0.129, full rotation occurs with a period of 227.0 psec. These results are in very good agreement with the data from [31].

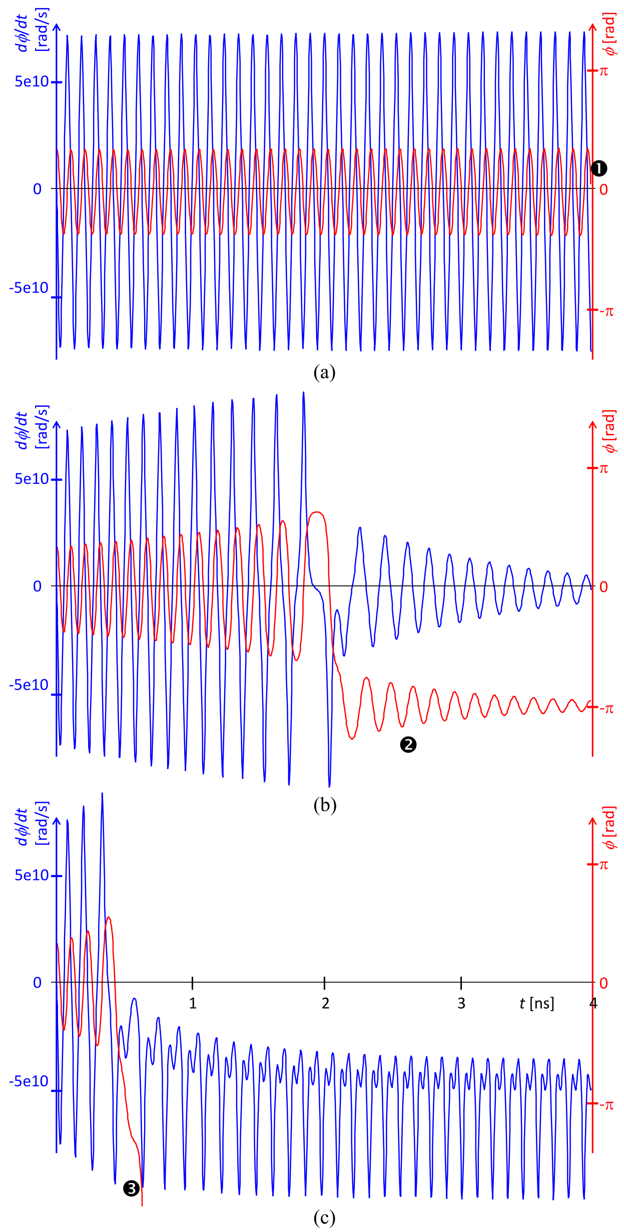

Fig. 5. Small field case. STO simulations according to (8): (a)–(c) are the angle ϕ and the angular velocity $d\phi/dt$ vs time. The initial angle $\phi_0 = 65^\circ$, $\alpha = 1 \times 10^{-3}$, $\omega_a/(2\pi) = 1$ GHz, $r_h = 0.5$, $r_p = 100$. The absolute value of the current excitation increases: ① $r_u = -0.06$ (small oscillations around $\phi = 0$), ②$r_u = -0.10$ (the trajectory ends at the stable point $\phi = -\pi$ rads), ③$r_u = -0.22$ (full rotation).

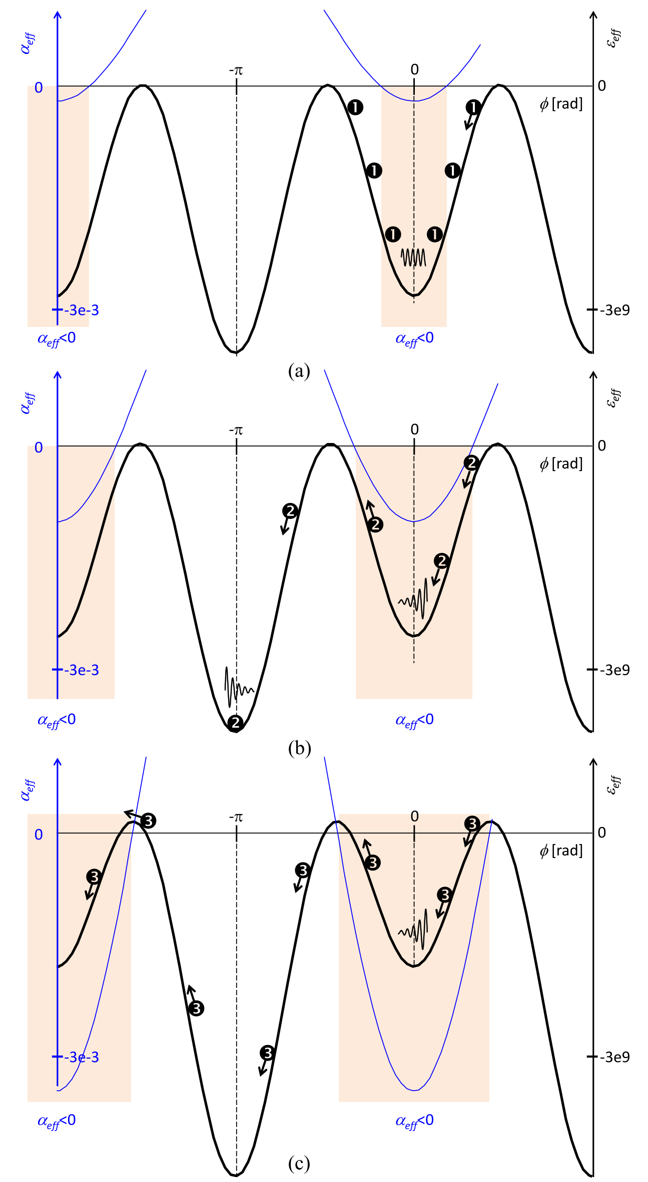

Fig. 6. Effective particle movements in potential profiles. The variants (a)–(c) correspond to the oscillation modes of Fig. 5(a)–(c). The region with negative damping allows small oscillations ①or causes the particle to be forced out into adjacent well ②with stable equilibrium point $\phi = -\pi$ rads, or accelerates the particle such that it overcomes also this well, and full rotations occur ③.

Disclosing the memristive character of damping allows studying interesting aspects of the STO with the knowledge from the field of memristive systems. For example, the application of memristor fingerprints to the friction coefficient $\alpha_{\text{eff}}(\phi)$ reveals that, under conditions as in [37], the mechanical counterparts of the memristor voltage and current in the electrical STO model must draw odd-symmetric hysteretic loops. These counterparts are angular velocity $d\phi/dt$ and friction torque τ_{frict}. This is confirmed by the results in Fig. 7, where the parameters are set to the so-called large field case, i.e., $h > \omega_a + u^2/\omega_p$ [31].

The oscillation period in Fig. 7(a) stabilizes at 247.5 psec., and the pinched steady-state hysteresis loop is drawn in the friction torque vs angular velocity space. It is a type-I pinching with the loop shape typical for ideal memristors [38].

Another consideration is that the constitutive relation of memristive damping must be preserved in all circumstances for any STO mode including all transition processes. This constitutive relation holds between mechanical equivalents of electric flow and electrical charges, i.e., the rotational angle ϕ and the time integral of friction torque $\int \tau_{frict}\, dt$. It is known that the constitutive relation of electrical memristor can be obtained by integration of memductance with respect to flow [39]. Applying this to the rotary mechanical memristor, the constitutive relation

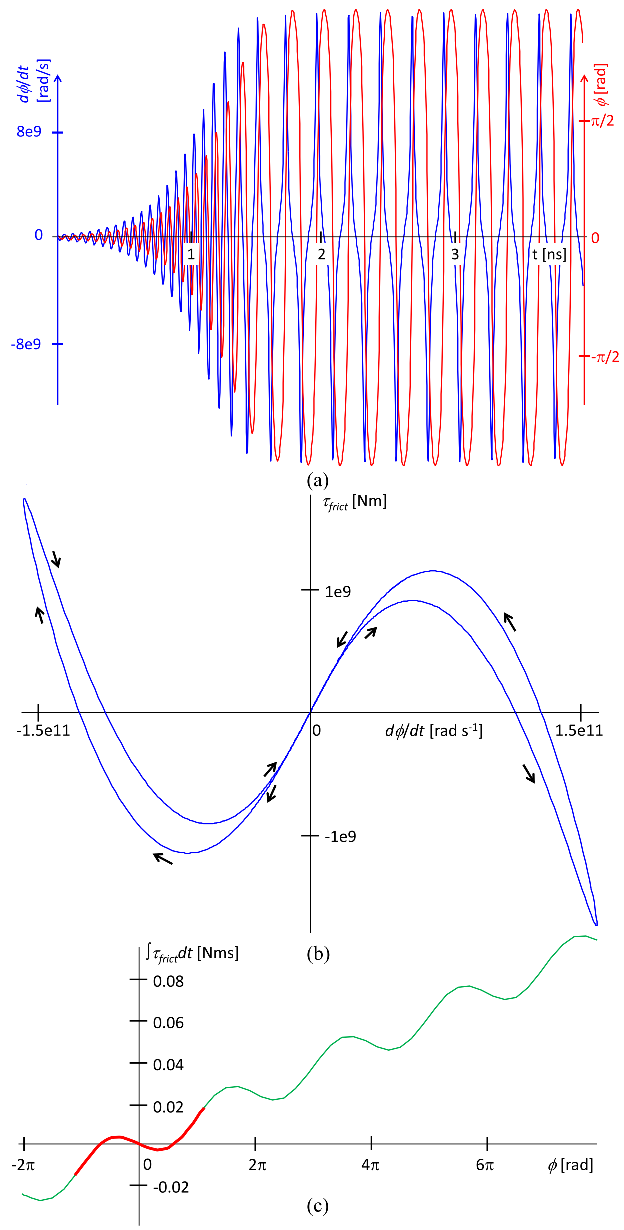

Fig. 7. Large field case. Initial angle $\phi_0 = 1^\circ, \alpha = 0.01, \omega_a/(2\pi) = 1$ GHz, $r_h = 1.4, r_p = 100, r_u = -1.1$. (a) Waveforms of angle ϕ and angular velocity $d\phi/dt$. (b) The friction torque vs angular velocity exhibits a typical memristive pinched hysteresis loop. (c) The time integral of friction torque vs angle is unambiguous in all circumstances, exhibiting the features of the constitutive relation of the memristor. The marked section is the working area of the oscillator when transitioning to the steady state.

will be in the form

$$\int \tau_{frict}(\phi)\, dt = \int G_M(\phi)\, d\phi = \alpha t + 2\frac{r_u}{r_p}\cos\phi + C \quad (9)$$

where C is the constant of integration. Fig. 7(c) fully confirms this consideration.

Note that two characteristics in Fig. 7(b) and (c) provide different views of the same object, namely the memristor, from two different floors of the storeyed structure in Fig. 2.

V. Conclusion

The paper refers to the importance of the so-called predictive models of nanodevices. The main feature of these models is their ability to mimic the behavior of the original independently of the way the model is included in the external environment. A number of current models of nanodevices lack this ability, particularly because the rules of the correct modeling from [6] have not been considered consistently. The methodology described in the paper starts from a generalization of Chua's table and storeyed structure to the Across-Through space. It enables identification of the so-called models with mistaken identity and their replacement by predictive models. The procedure is illustrated on the example of spin-torque nano-oscillator, namely how the nonlinear differential equation of motion of the analyzed system can be used for the synthesis of its predictive model, compounded from nonlinear fundamental elements from Chua's table, and how such a model can be used for revealing the mechanisms of the system operation in various modes. Specifically for the spin-torque oscillator, the new piece of knowledge, acquired from this approach, is that the spin-transfer torque effect, caused by the current flowing through the magnetic element, modifies the natural magnetic damping torque by a mechanism that can be considered as the operation of a hidden locally active memristor.

References

[1] L. Chkhartishvilli *et al.*, "How to calculate nanocapacitance," *Amer. J. Nano Res. Appl.*, vol. 5, no. 3–1, pp. 9–12, 2017.
[2] Y. Miyamoto, A. Rubio, S. G. Louie, and M. L. Cohen, "Self-inductance of chiral conducting nanotubes," *Phys. Rev. B*, vol. 60, no. 19, pp. 13885–13889, Nov. 15, 1999.
[3] D. B. Strukov, G. S. Snider, D. R. Stewart, and R. S. Williams, "The missing memristor found," *Nature*, vol. 453, pp. 80–83, 2008.
[4] M. D. Pickett, *et al.*, "Switching dynamics in titanium dioxide memristive devices," *J. Appl. Phys.*, vol. 106, 2009, Art. no. 074508.
[5] D. Ielmini, "Modeling the universal set/reset characteristics of Bipolar RRAM by field- and temperature-driven filament growth," *IEEE Trans. Electron Devices*, vol. 58, no. 12, pp. 4309–4317, Oct. 6, 2011.
[6] L. O. Chua, "Nonlinear circuit foundations for nanodevices, Part I: The four-element torus," *Proc. IEEE*, vol. 91, no. 11, pp. 1830–1859, Nov. 2003.
[7] L. O. Chua, "Local activity is the origin of complexity," *Int. J. Bifurcation Chaos*, vol. 15, no. 11, pp. 3435–3456, 2005.
[8] L. O. Chua, "Memristor, Hodgkin-Huxley, and EDGE OF CHaos," *Nanotechnology*, vol. 24, no. 38, 2013, Art. no. 383001.
[9] L. O. Chua, "Device modeling via basic nonlinear circuit elements," *IEEE Trans. Circuits Syst.*, vol. CAS-27, no. 11, pp. 1014–1044, Nov. 1980.
[10] L. O. Chua, V. Sbitnev, and H. Kim, "Hodgkin-Huxley axon is made of memristors," *Int. Bifurcation Chaos*, vol. 22, no. 3, 2012, Art. no. 1230011.
[11] X. Duan, Y. Huang, and C. M. Lieber, "Nonvolatile memory and programmable logic from molecule-gated nanowires," *Nano Lett.*, vol. 2, no. 5, pp. 487–490, 2002.
[12] B. D. Josephson, "Possible new effects in superconductive tunneling," *Phys. Lett.*, vol. 1, pp. 251–253, 1962.
[13] L. Chua and Y.-F. Lam, "A theory of algebraic n-ports," *IEEE Trans. Circuit Theory*, vol. CT-20, no. 4, pp. 370–382, Jul. 1973.
[14] M.-S. Abdelouahab, R. Lozi, and L. Chua, "Memfractance: A mathematical paradigm for circuit elements with memory," *Int. J. Bifurcation Chaos*, vol. 24, no. 9,2014, Art. no. 1430023.
[15] B. S. Sreeja and S. Radha, "Fabrication and characterization of high-q nano-inductor for power electronics," *Bonfring Int. J. Power Syst. Integr. Circuits*, vol. 1, pp. 43–47, 2011.
[16] S. Lu, Y. Sun, M. Goldberg, D. R. Zimmanck, and C. R. Sullivan, "30-MHz Power inductor using nano-granular magnetic material," in *Proc. IEEE Power Electron. Spec. Conf.*, Orlando, FL, USA, Jun. 2007, pp. 1773–1776.

[17] Y. Xu, X. Xie, Y. Duan, L. Wang, Z. Cheng, and J. Cheng, "A review of impedance measurements of whole cells," *Biosensors Bioelectron.*, vol. 77, pp. 824–836, 2016.
[18] A. Gebregergis, P. Pillay, and R. Rengaswamy, "PEMFC fault diagnosis, modeling, and mitigation," *IEEE Trans. Ind. Appl.*, vol. 46, no. 1, pp. 295–303, Jan./Feb. 2010.
[19] J. Bisquert, G. G-Belmonte, P. Bueno, E. Longo, and L. O. S. Bulhões, "Impedance of constant phase element (CPE)-blocked diffusion in film electrodes," *J. Electroanalytical Chem.*, vol. 452, pp. 229–234, 1998.
[20] A. L. Hodgkin and A. F. Huxley, "A quantitative description of membrane current and its application to conduction and excitation in nerve," *J. Physiol.*, vol. 117, pp. 500–544, 1952.
[21] L. O. Chua, "Resistance switching memories are memristors," *Appl. Phys. A*, vol. 102, pp. 765–783, 2011.
[22] L. O. Chua, "If it's pinched it's a memristor," *Semicond. Sci. Technol.*, vol. 29, 2014, Art. no. 104001.
[23] L. O. Chua and S. M. Kang, "Memristive devices and systems," *Proc. IEEE*, vol. 64, no. 2, pp. 209–223, Feb. 1976.
[24] L. O. Chua, "Memristor—the missing circuit element," *IEEE Trans. Circuit Theory*, vol. CT-18, no. 5, pp. 507–519, Sept. 1971.
[25] L. Chua, "Everything you wish to know about memristors but are afraid to ask," *Radioengineering*, vol. 24, no. 2, pp. 319–368, 2015.
[26] F. Corinto, P. P. Civalleri, and L. O. Chua, "A theoretical approach to memristor devices," *IEEE J. Emerg. Sel. Topics Circuits Syst.*, vol. 5, no. 2, pp. 123–132, 2015.
[27] M. E. Fouda, A. S. Elwakil, and A. G. Radwan, "Pinched hysteresis with inverse-memristor frequency characteristics in some nonlinear circuit elements," *Microelectron. J.*, vol. 46, pp. 834–838, 2015.
[28] C. Si *et al.*, "An ion signal responsive dynamic protein nano-spring constructed by high ordered host-guest recognition," *Chem. Commun.*, vol. 52, no. 14, pp. 2924–2927, 2016.
[29] P. G. Yot *et al.*, "Metal–organic frameworks as potential shock absorbers: the case of the highly flexible MIL-53(Al)," *Chem. Commun.*, vol. 50, pp. 9462–9464, 2014.
[30] J. C. Meyer, M. Paillet, and S. Roth, "Single-Molecule Torsional Pendulum," *Science*, vol. 309, pp. 1539–1541, 2005.
[31] Ya. B. Bazaliy and F. Arammash, "Planar approximation for the frequencies of spin transfer oscillators," *Phys. Rev. B*, vol. 84, no. 13, Oct. 5, 2011, Art. no. 132404.
[32] D. Biolek, Z. Biolek, and V. Biolkova, "Memristors and other higher-order elements in generalized through-across domain," in *Proc. 2016 Int. IEEE Conf. Electron. Circuits Syst.*, 2016, pp. 604–607.
[33] D. Biolek, Z. Biolek, and V. Biolkova, "Spice modeling of memristive, memcapacitative and meminductive systems," in *Proc. Eur. Conf. Circuit Theory Des.*, Antalya, Turkey, 2009, pp. 249–252.
[34] M. C. Smith, "Synthesis of mechanical networks: The inerter," *IEEE Trans. Automat. Control*, vol. 47, no. 10, pp. 1648–1662, Oct. 2002.
[35] D. Biolek, Z. Biolek, and V. Biolkova, "Every nonlinear element from Chua's table can generate pinched hysteresis loops: Generalised homothety theorem," *Electron. Lett.*, vol. 52, no. 21, pp. 1744–1746, 2016.
[36] G. F. Oster and D. M. Auslander, "The memristor: A new bond graph element," *J. Dyn. Sys., Meas., Control*, vol. 94, no. 3, pp. 249–252, 1972.
[37] D. Biolek, Z. Biolek, and V. Biolkova, "Pinched hysteretic loops of ideal memristors, memcapacitors and meminductors must be 'self-crossing'," *Electron. Lett.*, vol. 47, no. 25, pp. 1385–1387, 2011.
[38] Z. Biolek and D. Biolek, "How can the hysteresis loop of the ideal memristor be pinched?," *IEEE Trans. Circuits Syst. II, Express Briefs*, vol. 61, no. 7, pp. 491–495, Jul. 2014.
[39] Z. Biolek, D. Biolek, and V. Biolkova, "Analytical solution of circuits employing voltage- and current-excited memristors," *IEEE Trans. Circuits Syst. I, Reg. Papers*, vol. 59, no. 11, pp. 2619–2628, Nov. 2012.

Dalibor Biolek (M'99–SM'15) received the M.Sc. degree in electrical engineering from Brno University of Technology, Brno, Czech Republic, in 1983, and the PhD. degree in electronics from the Military Academy Brno, Brno, Czech Republic, in 1989, focusing on algorithms of the symbolic and numerical computer analyses of electronic circuits with a view to the linear continuous-time and switched filters.

He is currently with the Department of EE, University of Defence Brno (UDB), Brno, Czech Republic, and with the Department of Microelectronics, Brno University of Technology (BUT), Brno, Czech Republic. His scientific activity is directed to the areas of general circuit theory, frequency filters, mem-systems, and computer simulation of electronic systems. He has authored and coauthored more than 400 papers and is author of several books on circuit analysis and simulation. He is currently a Professor with BUT and UDB in the field of theoretical electrical engineering.

Prof. Biolek is a Member of the CAS/COM Czech National Group of IEEE. He is currently an Associate Editor of *Electronics Letters*.

Zdeněk Biolek was born in Ostrava, Czech Republic, in 1959. He received the PhD. degree in electronics and informatics from Brno University of Technology, Brno, Czech Republic, in 2001.

He is currently with the Department of Microelectronics, Brno University of Technology, Brno, Czech Republic. Until the year 1993, he was an Independent Researcher in semicon-ductor company TESLA Rožnov. He is the author of unique electronic instruments associated with IC production and testing. He is also the author of several papers from the area of the utilization of variational principles in theoretical electrical engineering and stability testing of resistive circuits, and also from the field of memristors and mem-systems. He is also the co-author of two books about memristive systems and PSpice modeling and simulation of special electronic circuits including switched-capacitor filters, switched dc–dc converters, and memristors.